In Vivo Real-Time 3-D Intracardiac Echo Using PMUT Arrays

David E. Dausch, Kristin H. Gilchrist, James B. Carlson, Stephen D. Hall, John B. Castellucci, and Olaf T. von Ramm

***Abstract*—Piezoelectric micromachined ultrasound transducer (PMUT) matrix arrays were fabricated containing novel through-silicon interconnects and integrated into intracardiac catheters for *in vivo* real-time 3-D imaging. PMUT arrays with rectangular apertures containing 256 and 512 active elements were fabricated and operated at 5 MHz. The arrays were bulk micromachined in silicon-on-insulator substrates, and contained flexural unimorph membranes comprising the device silicon, lead zirconate titanate (PZT), and electrode layers. Through-silicon interconnects were fabricated by depositing a thin-film conformal copper layer in the bulk micromachined via under each PMUT membrane and photolithographically patterning this copper layer on the back of the substrate to facilitate contact with the individually addressable matrix array elements. Cable assemblies containing insulated 45-AWG copper wires and a termination silicon substrate were thermocompression bonded to the PMUT substrate for signal wire interconnection to the PMUT array. Side-viewing 14-Fr catheters were fabricated and introduced through the femoral vein in an adult porcine model. Real-time 3-D images were acquired from the right atrium using a prototype ultrasound scanner. Full 60° × 60° volume sectors were obtained with penetration depth of 8 to 10 cm at frame rates of 26 to 31 volumes per second.**

I. Introduction

The use of 3-D echo is increasing for many interventional cardiovascular procedures such as transcatheter aortic valve intervention and percutaneous mitral valve repair. Advantages of 3-D echo compared with 2-D include more accurate assessment of valve annulus for prosthesis sizing [1] as well as more intuitive views for intraprocedural guidance and repair of paravalvular leak [2], [3]. Three-dimensional transesophageal echo (TEE) is the most ubiquitous choice for intraprocedural 3-D imaging and generally provides adequate imaging; however; procedural logistics are more complicated. Because TEE requires general anesthesia and esophageal intubation, additional personnel including an anesthesiologist and an echocardiographer must be present for the procedure, and patient risk and discomfort are increased [3], [4]. Technical limitations of 3-D TEE include reduced resolution for anterior structures, limited frame rate for full volume images, imaging artifacts, and tissue dropout caused by shadowing [3], [5]–[8].

Three-dimensional intracardiac echo (ICE) would overcome many of these challenges. ICE provides a catheter-based interventional imaging tool that does not require general anesthesia, patient intubation, or additional imaging personnel. ICE imaging also allows targets to be viewed in the near field from the right atrium with better resolution compared with TEE and transthoracic echo [4], [9], [10]. Real-time 3-D ICE catheters have recently become commercially available (AcuNav V, Siemens Medical, Malvern, PA) [11]; however, these catheters do not contain matrix arrays, and only partial volumes can be acquired at limited frame rate (e.g., 60° × 15° at 20 volumes per second) which limits the targets that can be imaged adequately. The maximum volume sector for AcuNav V is 90° × 22° [12], which produces an elevation width of only 15 mm at 40 mm depth. This is an inadequate sector size for imaging of, for example, the aortic valve with annulus of 20 to 25 mm. Three-dimensional TEE probes do contain matrix phased arrays and can produce a full 60° × 60° volume, but with limited frame rate of 7 to 10 volumes per second [5]. TEE requires a deeper scan resulting in larger overall volume imaged compared with ICE, which reduces frame rate for the larger sector scans. Mechanically scanned linear phased arrays were assembled in ICE catheters producing a volume sector of 86° × 57° at 6 cm depth but with a frame rate of less than 6 volumes per second [13]. High frame rate is required for adequate imaging of cardiac structural dynamics.

ICE catheters with matrix or ring arrays have been reported in the literature for some years. *In vivo* 3-D imaging was demonstrated with 12-Fr and 7-Fr ICE catheters containing side-viewing PZT matrix arrays operating at 5 MHz with 64 and 112 elements, respectively [14], [15]. Image quality was limited, however, likely because of the small array apertures and low element count. A capacitive micromachined ultrasound transducer (CMUT) ring array operating at 10 MHz with 64 elements and diameter of 2.5 mm was used to produce an *in vivo* 3-D image of the endocardial surface of a porcine heart, but with limited image quality and scan depth of only 1 cm [16]. CMUT matrix arrays have been reported with 256 elements [17]; however, the overall device size was 6 × 10 mm and was not compatible with catheter packaging.

This paper reports a novel PMUT device construction containing through-silicon interconnects that enabled matrix phased arrays with up to 512 elements to be integrated into intracardiac catheters for real-time 3-D imaging.

Manuscript received April 11, 2014; accepted June 20, 2014.

D. E. Dausch, K. H. Gilchrist, J. B. Carlson, and S. D. Hall are with the Electronics and Applied Physics Division, RTI International, Research Triangle Park, NC (e-mail: dausch@rti.org).

J. B. Castellucci and O. T. von Ramm are with the Department of Biomedical Engineering, Duke University, Durham, NC.

DOI http://dx.doi.org/10.1109/TUFFC.2014.006452

Through-silicon interconnects have been used with CMUT arrays to integrate the transducers with other integrated circuitry [17], [18]. PZT matrix arrays have also been fabricated on silicon multilayer interconnect circuits but required rigid substrate length of nearly 5 cm [19]. Several recent reports have also demonstrated PMUT matrix arrays, including previous work from the authors [20]–[23]; however, extensive fan-out of electrical leads prevents integration in a reasonably sized probe or catheter. This work is the first report to our knowledge of the use of through-silicon interconnects in the substrate of a PMUT array, enabling high-density matrix arrays to be integrated directly with catheter cabling without significant increase of the matrix array footprint. ICE catheters with 14 Fr diameter were fabricated and introduced through the femoral vein and into the right atrium in a live porcine model to produce real-time 3-D intracardiac ultrasound images.

II. Methods

A. PMUT Fabrication

PMUT arrays were fabricated in silicon wafers and consisted of piezoelectric unimorph membranes that formed the active transducer elements. An overall device schematic is shown in Fig. 1. PMUTs were fabricated on 100-mm-diameter silicon-on-insulator wafers with silicon device layer thickness of 5 μm, buried SiO_2 layer of 1 μm, and bulk silicon substrate of 400 μm thickness. Conductive plugs were formed in the device silicon layer by etching through the device silicon layer and plating platinum metal to fill the plugs. Prior to plating, thermal SiO_2 with 1 μm thickness was grown on the wafer surface and on the plug sidewalls. The surface of the wafer was then polished using a chemo-mechanical polish to remove the plating overburden. The process for platinum plug fabrication was described previously [24]. The plugs served as a conductive path from the transducer bottom electrode through the device silicon layer to the through-substrate metallization.

The piezoelectric stack layers were then deposited, including a Ti/Pt bottom electrode, $Pb(Zr_{0.52},Ti_{0.48})O_3$ film, Ti/Au top electrode, and an interelement benzocyclobutene (BCB) dielectric film. The PZT film was spin coated and crystalized at 700°C using a metalorganic decomposition process from an acetate precursor solution [25]. The resulting PZT film thickness was 1 μm. The PZT was patterned using a wet chemical etch [26] to form individual piezoelectric elements. The bottom Ti/Pt electrode was patterned using ion milling to electrically isolate each element. The top Ti/Au layer provided a planar ground electrode. The device silicon substrate was also etched down to the buried SiO_2 around each element to ensure electrical isolation between elements. The piezoelectric stack and platinum plug features are shown in Figs. 2(a) and 2(b).

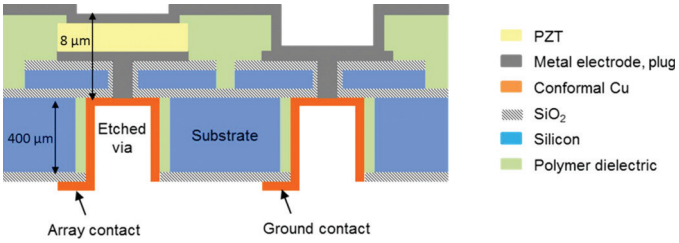

Fig. 1. Cross-sectional schematic diagram of a PMUT device with through-silicon interconnect. Schematic shows a transducer element with PZT layer and a ground contact pad containing no PZT. Combined electrode, PZT, device silicon membrane thickness is approximately 8 μm, and substrate thickness is 400 μm. This schematic is not to scale in either height or width dimensions.

Through-silicon interconnects were formed to provide interconnection to both signal and ground contacts from the back side of the silicon substrate. Through-substrate vias were etched directly under each PZT element using deep reactive ion etching (DRIE). A parylene dielectric layer was deposited conformally in the etched vias to cover the via sidewalls. A conformal copper layer with thickness

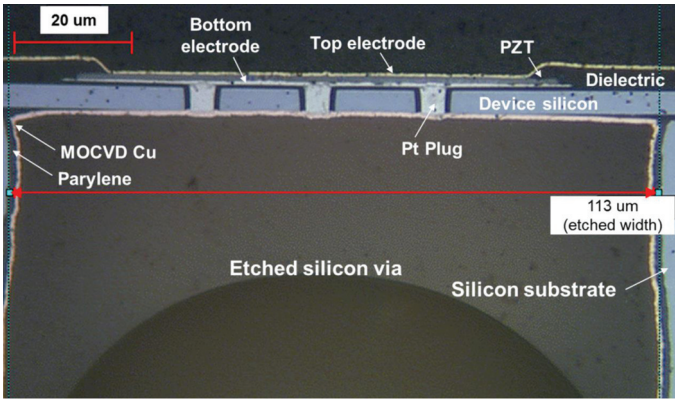

(a)

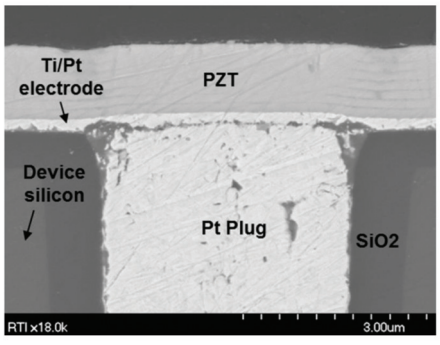

(b)

Fig. 2. (a) Cross-sectional microscope image of a PMUT membrane. Electrical connection for each element is formed between the bottom electrode, the platinum plug, and the MOCVD copper layer deposited in the etched silicon substrate via. (Note: The domed feature at the bottom of the image is a bubble artifact from the potting epoxy used to fill the etched via for polishing to create a smooth cross section for the image. Potting epoxy is not part of the final operational PMUT.) (b) Cross-sectional scanning electron microscope image with magnified view of the PZT-to-Pt plug junction.

of 2 μm was deposited by metalorganic chemical vapor deposition (MOCVD) such that it made electrical contact at the tops of the silicon vias with the platinum plugs connected to the patterned platinum bottom electrodes. The copper layer was patterned and etched on the back side of the Si substrate to form individual electrical contacts to each PZT element. To connect the top ground electrode, separate ground contacts were formed by etching the PZT layer away such that the top gold and bottom platinum electrodes were in contact to create an electrical path for the ground layer to the back side of the substrate. This construction allowed all of the electrical contacts to be formed on the back side of the silicon substrate such that no additional electrical contacts were necessary using wirebonding or other methods that would increase the matrix array footprint.

B. Cabling and Interconnection

Cable interconnection compatible with the silicon-based transducer devices was also developed. For a matrix phased array with up to 512 elements that must fit inside a small-diameter catheter, conventional wiring approaches such as coaxial or flex cables cannot be used because of the limited interconnect density. Cable assemblies were fabricated with signal wires attached to each transducer element that fit within a cross-sectional diameter of less than 3 mm, and these assemblies were interconnected directly to the PMUT substrates. CMUT arrays have been integrated with CMOS circuitry containing amplification and multiplexing functions [27]. This enables reduction in the wire count within the catheter; however, it is also required for CMUT devices because of the high impedance of these transducer elements and poor impedance match to cabling with high capacitance. Even bulk PZT matrix array transducer elements have impedance match challenges resulting from the lower capacitance and associated high impedance of the elements. Because PMUT devices contain a thin-film piezoelectric layer, element capacitance is higher than for other transducer types, which allows direct connection to wiring with acceptable impedance match. This obviates the need for amplification and multiplexing circuitry. PMUT element impedance is discussed in the results section.

Cable assemblies were constructed from individual 45-AWG copper wires with polyurethane-nylon insulation. A silicon wire termination substrate was fabricated by etching through-holes in a silicon substrate with an array footprint and pitch that matched the patterned copper pads on the back surface of the PMUT array. This provided the distal cable termination to the PMUT array elements. The copper wires were inserted into the silicon termination substrate and fixed in place using a low-viscosity epoxy. The surface of the substrate was polished to expose the ends of the copper wire and then placed in a gold electroplating solution to coat the ends of the wires. The wire substrate and PMUT substrate were thermocompression bonded using a flip-chip bonder (FC150, Karl Suss, Garching, Germany) with an underfill epoxy such that the wire ends were aligned with and connected to the copper pads on the PMUT substrate corresponding to each individual PMUT element; that is, the electric connection comprised one copper wire per PMUT element. Bond yield was typically 95% or greater of the array elements connected to their respective wires. The cable assembly was encapsulated in polyolefin shrink tubing. The outer diameter of a cable assembly containing 512 signal wires and 128 ground wires averaged 2.8 mm, which easily fit in the catheter lumen with an inner diameter of 3.8 mm (11 Fr). Because the cable consisted of individual wires as opposed to ribbons or other more rigid cable, the wire bundle remained fully flexible to allow easy insertion into the catheter shaft and did not impede catheter tip deflection. Fig. 3 shows a schematic diagram of the wire substrate and a PMUT array bonded to a cable assembly with 256 signal wires and 128 ground wires. At the distal end of the assembly, the thickest portion of the PMUT/termination substrate/wire bundle stack measured 2.9 mm width × 2.5 mm height, and the final length of the rigid array assembly was approximately 15 mm. PMUT die size was 11.8 mm × 2.5 mm. The proximal end of the cable was solder terminated to standard printed circuit boards containing connectors to the ultrasound system cable. The overall signal cable length from transducer tip to termination boards was 137 cm.

Ground wires were interspersed to provide some crosstalk isolation by twisting together two to four signal wires with each ground wire. Crosstalk measurement was not performed on catheter devices in this study; however, two cable test assemblies were made with interspersed grounds and non-interspersed grounds, respectively, for comparison. The assemblies contained 128 signal wires and 32 ground wires for connection to a 32 × 4 PMUT test array operating at 5 MHz. B-mode images were obtained using the 32-element azimuth aperture consisting of 0.175 mm interelement pitch for overall aperture of 5.6 mm. Each of the 128 PMUT elements were connected to separate transmit/receive channels on the T5 phased-array ultrasound system (Duke University, Durham, NC). As shown in Fig. 4, images of a sponge placed above string targets were obtained in a water tank with each of the cable assemblies connected to the 32 × 4 element PMUT array. Fig. 4(a) shows the image obtained when the array was connected to the cable with non-interspersed ground wires. Significant crosstalk was observed, as manifested by the much brighter signal in the center of the image compared with the weaker signal at wider sector angles, as well as the non-uniform spacing between the string targets. These observations suggested poor array phasing caused by crosstalk between the signal wires. When the array was attached to the cable assembly with interspersed ground wires, the image shown in Fig. 4(b) showed improved phasing with more uniform signal intensity across the sector scan and uniform string spacing. This result increased confidence that a PMUT array with catheter cabling could produce sufficient image quality for this study.

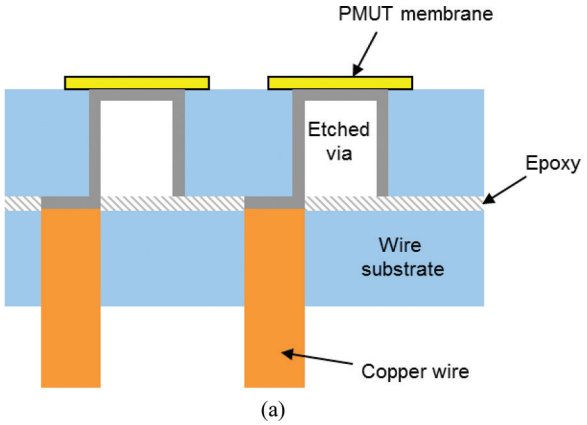

(a)

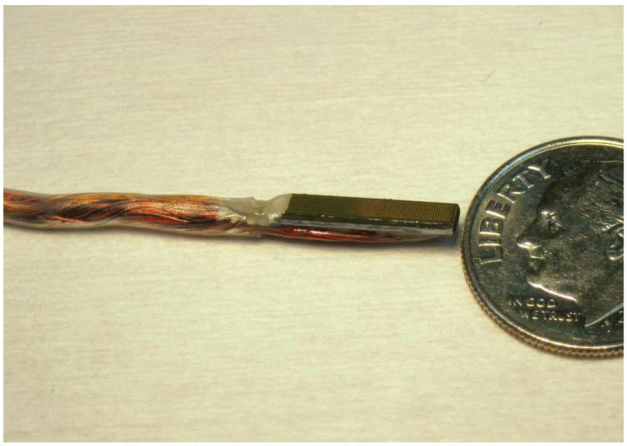

(b)

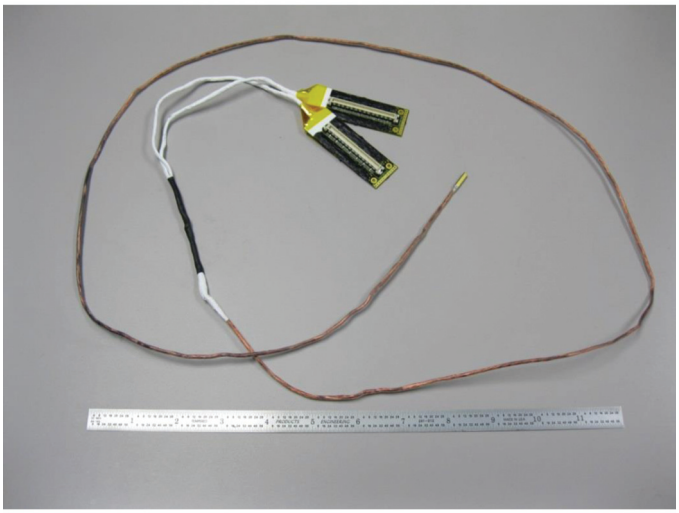

(c)

Fig. 3. (a) Cross-sectional schematic of a PMUT array substrate bonded to a signal wire substrate. (b) Photograph of a matrix PMUT array containing 256 active elements (64 × 16 PMUT membranes) interconnected to the distal end of a cable assembly containing 256 signal wires and 128 ground wires. The distal end of the pMUT/termination substrate/wire bundle assembly measured 2.9 mm width × 2.5 mm height × 15 mm length. (c) Photograph of the full PMUT-cable assembly measuring 137 cm in length.

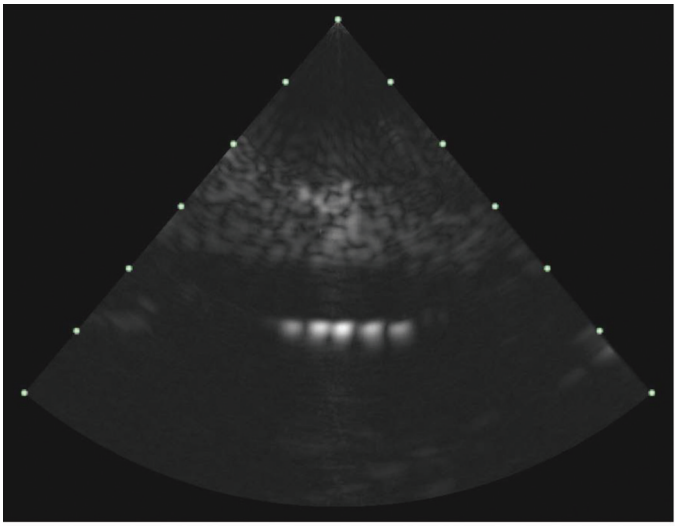

(a)

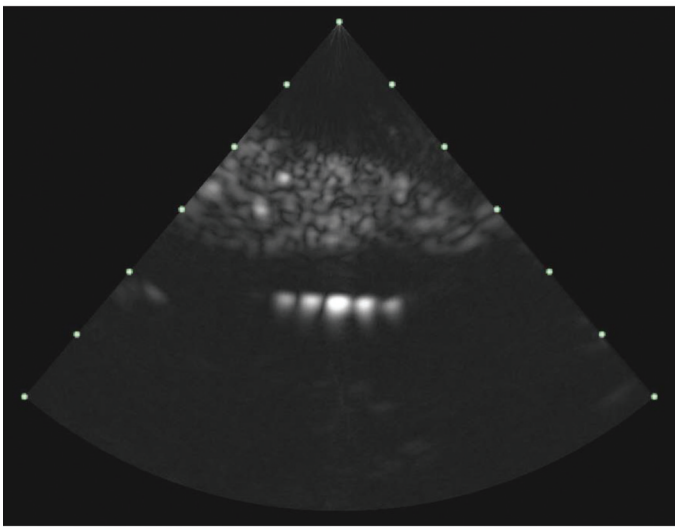

(b)

Fig. 4. B-mode images of a sponge with triangular cross section placed over nylon strings in a water tank. Images made using the Duke T5 scanner. String spacing was 2.8 mm. Images were acquired using a 32 × 4 PMUT test array operating at 5 MHz connected to two different cable assemblies: (a) cable with non-interspersed ground wires, and (b) cable assembly with interspersed grounds.

C. Catheter Construction

Prototype ICE catheters were fabricated containing PMUT arrays with interconnected cable assemblies. Catheter shafts were fabricated by CarTika Medical Inc. (Maple Grove, MN), containing a braided polyether block amide (Pebax) outer wall, a fluoroscopic marker band, a stainless steel pull wire assembly for catheter tip deflection to ±90° (i.e., single-axis, bi-directional steering), and a steering handle to deflect the catheter tip. Catheter outer diameter was 4.5 mm (approximately 14 Fr), and working length was 90 cm. The transducer cable was threaded into the main lumen of the catheter shaft with inner diameter of 3.8 mm (11 Fr). The transducer was configured as side-

viewing, which is the standard orientation for ICE catheters placed in the right atrium for intracardiac imaging. A clear Pebax tube with inner diameter of approximately 4.2 mm was attached to the distal end of the catheter to cover the PMUT array, and easily accommodated the tip of the PMUT–cable assembly. The catheter lumen was filled with deionized water before imaging to provide the acoustic transmission path from the PMUT elements to the blood stream. No additional matching or backing layers were used for the PMUT array. Stopcock valves and polyimide tubing were attached to the proximal end of the catheter for water filling.

D. Transducer Testing and Imaging

Measurement of transducer elements was obtained from the transducer-cable assemblies by placing the transducer in a tank filled with deionized water. Transmit pulses from single PMUT elements were measured by transmitting with a 3-cycle sine wave pulse at 30 V_{pp} into a calibrated hydrophone (GL-0200, Onda Corp., Sunnyvale, CA) placed at a 20 mm distance from the transducer. An oscilloscope (TDS 754A, Tektronix Inc., Beaverton, OR) was used to measure the output voltage without prior amplification.

Two different ultrasound systems were used for imaging experiments in this work. The T5 phased-array ultrasound system (Duke University) features up to 1024 transmit and receive channels. Up to 32:1 receive parallel processing can be employed on up to 8 transmit bursts per acquisition sequence, yielding up to 32 000 lines per volume, or B-mode images may be acquired at rates in excess of 1000 frames per second. 15-bit detected data are generated before display. The real-time display system is based on an advanced nVidia graphics card (Quadro 6000, nVidia Corp., Santa Clara, CA) with 6 GB memory, 448 cores, 144 Gbps memory bandwidth, and 384-bit memory interface, which renders 1.3 billion triangles per second. When used with volumetric data, this enables multiple B-mode planes to be shown simultaneously, with or without a volume-rendered view. Orthogonal planes can be swept throughout the volume to obtain a clearer view of the targets of interest. The volume rendering can have arbitrary cut planes placed, with variable thickness. The zoom and rotation of the rendering can be adjusted in real time during scanning. T5 used minimal parallel processing for the data presented here, acquiring 8-cm-depth, 4000-line volumes at an 8 volumes per second rate, and 6-cm-depth B-modes at 69 frames per second. For this study, T5 was used only for water tank and phantom imaging.

To demonstrate *in vivo* animal imaging, a second portable ultrasound system was used for access to the animal surgery suite at Duke. The V360 prototype volume ultrasound scanner (Volumetrics Medical Imaging Inc., Durham, NC) uses up to 256 transmit and receive channels with up to 16:1 receive parallel processing. The system also has 256 additional transmit-only channels that were not used. B-scans can be generated at up to 72 frames per second, whereas volumes can be acquired at up to 60 volumes per second. For the data presented here at 8 cm scan depth, B-modes were acquired at 71 frames per second and 60° × 60° volumes at 31 volumes per second. 8-bit detected data are generated before display. Multiple planes, both B-mode and C-mode, can be displayed simultaneously by the hardware scan converter. These planes can be tilted at any angle and adjusted to any depth to examine any point within the volume. In place of the C-mode planes, a real-time volume rendering can be displayed with bounds set by two arbitrarily placed cut planes. A set of in-line, low-noise amplifiers was designed and built to increase the signal-to-noise level. These amplifiers were connected directly to the proximal end of the catheter, driving the signals down the system cabling and into the scanner. The T5 system did not require this extra amplification.

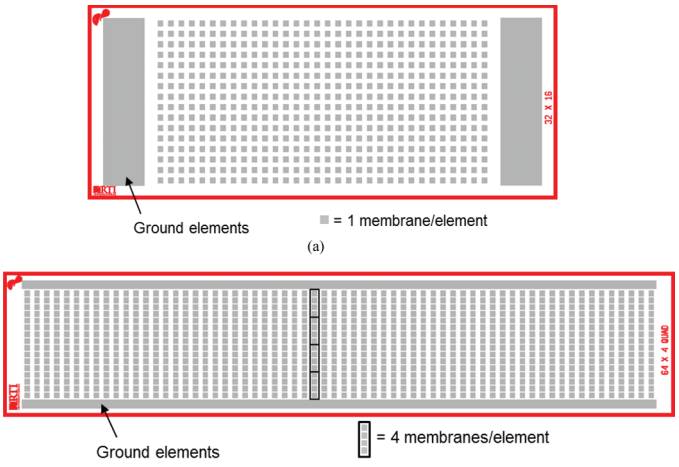

Fig. 5. Schematic layouts of (a) Array 1 containing 512 elements (32 × 16) in which each element comprised one membrane, and (b) Array 2 containing 256 elements (64 × 4) in which each element comprised four membranes.

III. Results

A. Matrix Array Configuration and In Vitro Testing

Two PMUT array configurations were incorporated into catheters as described in Table I. Element layouts of these arrays are shown in Fig. 5, and photographs of final assembled catheters are shown in Fig. 6. Rectangular apertures were chosen to take advantage of the side-viewing catheter orientation which allows wider azimuth aperture, whereas elevation aperture was constrained by catheter diameter. Array 1 contained 512 elements in a 32 × 16 arrangement, in which each array element contained one PMUT membrane. A PMUT membrane was defined by the etched via under each PZT element as shown previously. The dimensions of the etched membranes for both arrays were approximately 110 × 80 μm. This membrane size resulted in a transducer operating frequency of approximately 5 MHz, as described previously for flexure-

TABLE I. CATHETER PMUT ARRAY SPECIFICATIONS.

PMUT Array	Array 1	Array 2
Number of PMUT membranes (array)	512 (32 × 16)	1024 (64 × 16)
Number of transducer elements (array)	512 (32 × 16)	256 (64 × 4)
Number of PMUT membranes per element	1	4
Operating frequency (MHz)	5	5
Azimuth aperture (mm)	5.6	11.2
Azimuth pitch (mm)	0.175	0.175
Elevation aperture (mm)	2.8	1.9
Elevation pitch (mm)	0.175	0.48
Theoretical azimuth resolution, 4 cm depth (mm)	2.1	1.1
Theoretical elevation resolution, 4 cm depth (mm)	4.3	6.3

mode PMUT operation [28]. Pulse–echo imaging of a metal spring placed in a water tank is shown in Fig. 7 using the T5 ultrasound system. The PMUT elements were driven with 3-cycle sine wave pulses at 40 V_{pp} at 4.9 MHz. The catheter and spring were held in place, and T5 was used to rotate the displayed volume rendering in real time. These screen shots were obtained from the real-time volume rendering as it was rotated orthogonally and tilted at an angle to image the various angles of the spring.

PMUT Array 2 was configured in order maximize the azimuth aperture for improved azimuth resolution. The array contained 1024 PMUT membranes in a 64 × 16 arrangement. To demonstrate *in vivo* imaging, the V360 system was used, which contained only 256 transmit and receive channels. Thus, the 64 × 16 array was configured such that every 4 membranes in elevation were connected with a common copper pad on the back of the PMUT substrate to produce an array with 256 elements. This 64 × 4 arrangement preserved the 64-element azimuth aperture with some minimal elevation beam steering capability. As shown in Table I, the elevation aperture was also reduced to allow fabrication into smaller 12-Fr catheters in the future. One benefit of multiple membranes connected in parallel was the increase in element capacitance and decreased impedance for better matching to the signal cabling. Catheter signal wire capacitance to ground mea-

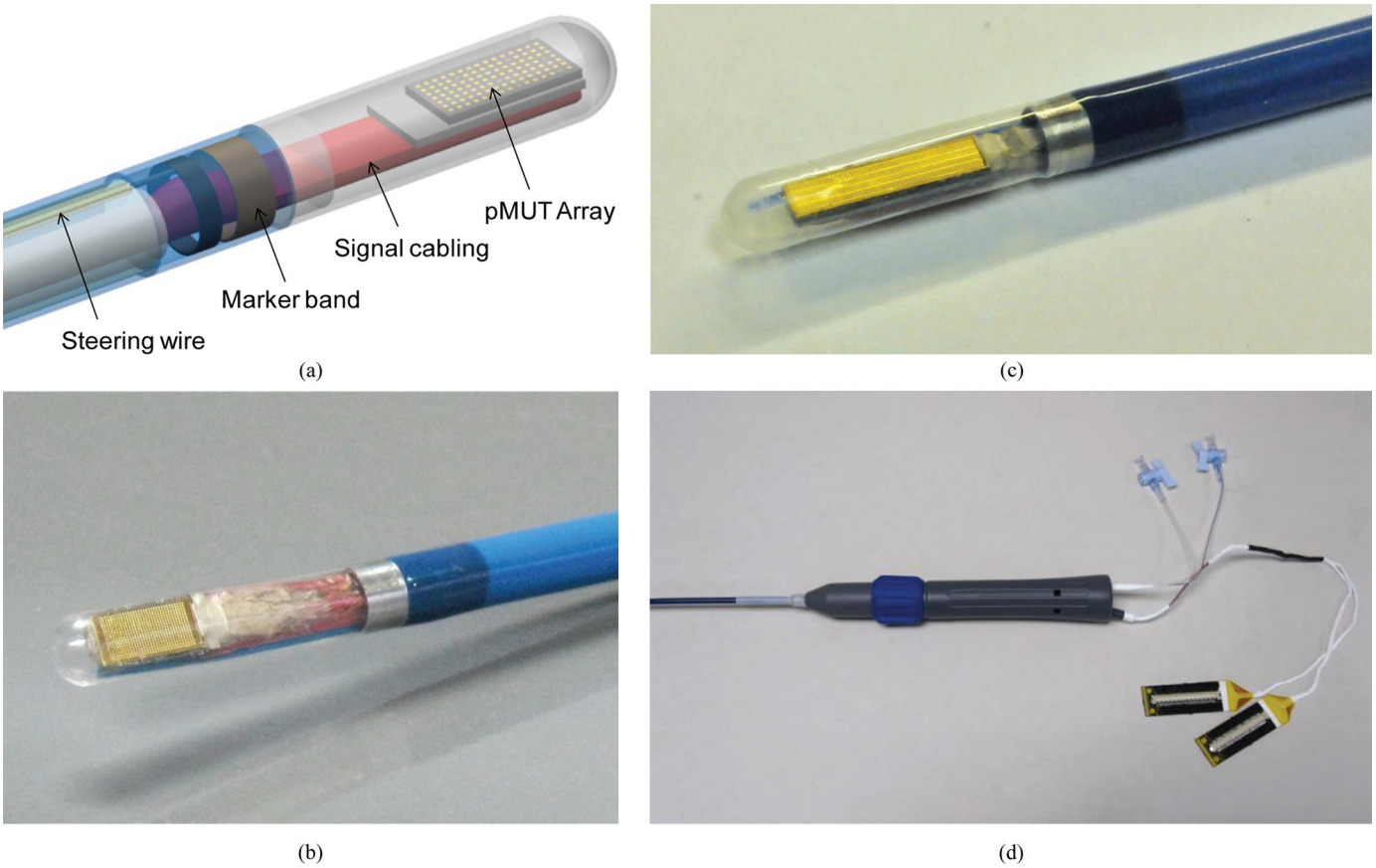

Fig. 6. (a) Mechanical model of the distal end of the steerable catheter. Photographs of the distal end of 14-Fr intracardiac catheters containing PMUT matrix arrays with (b) 512 elements (Array 1) and (c) 256 elements (Array 2). (d) The proximal end of the catheter containing a steering handle to deflect the tip, fluid fill lines and valves and termination connectors for connection to the ultrasound system cable.

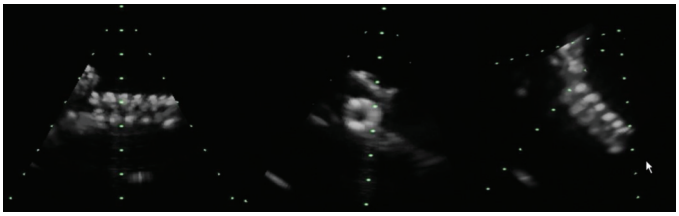

Fig. 7. Still frames captured from a real-time volume rendering of a metal spring held between a finger and thumb in a water tank using PMUT Array 1 operating at 4.9 MHz. The metal spring had outer coil diameter of 10 mm and wire diameter of 1 mm. Images of the spring include side (left image), through center (middle image), and oblique angle (right image) views. Each volume consists of more than 4000 lines acquired with the Duke T5 scanner. The real-time segment is provided as a multimedia attachment.

sured at 1 kHz was approximately 180 pF, whereas the capacitance of each pMUT membrane was 50 pF; therefore, increasing to four membranes per element increased element capacitance to 200 pF. This resulted in low element impedance of approximately 170 Ω at 5 MHz. In comparison, matrix array elements made from bulk PZT possess element impedance well into the kilohm range.

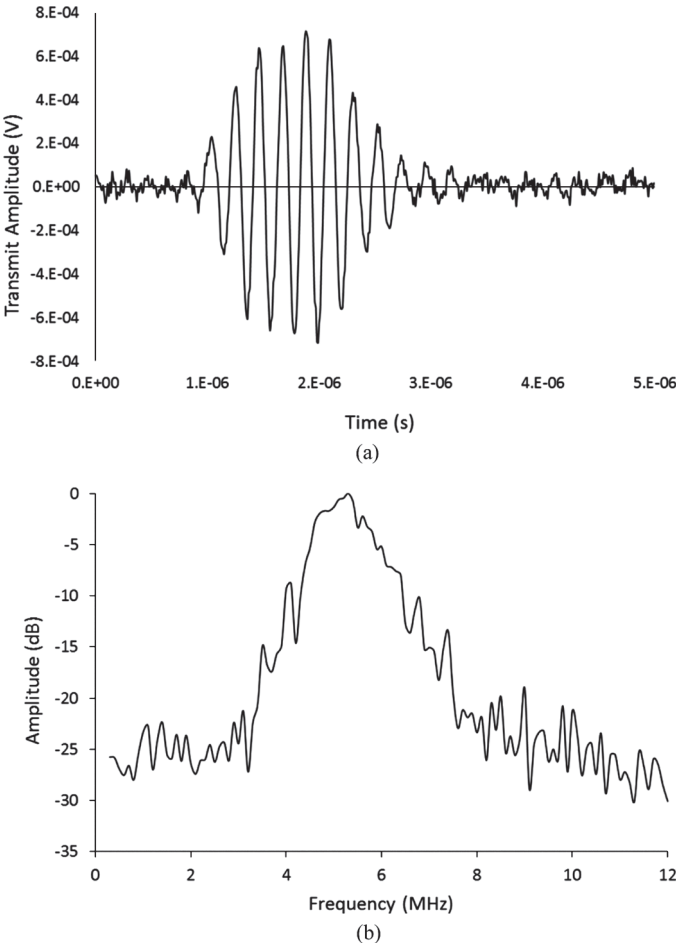

Fig. 8. (a) Transmit pulse from one element of PMUT Array 2 driven with a 3-cycle sine wave at 30 V_{pp} measured by a hydrophone without amplification at 20 mm distance. (b) FFT spectrum of transmit pulse with measured bandwidth of 30%.

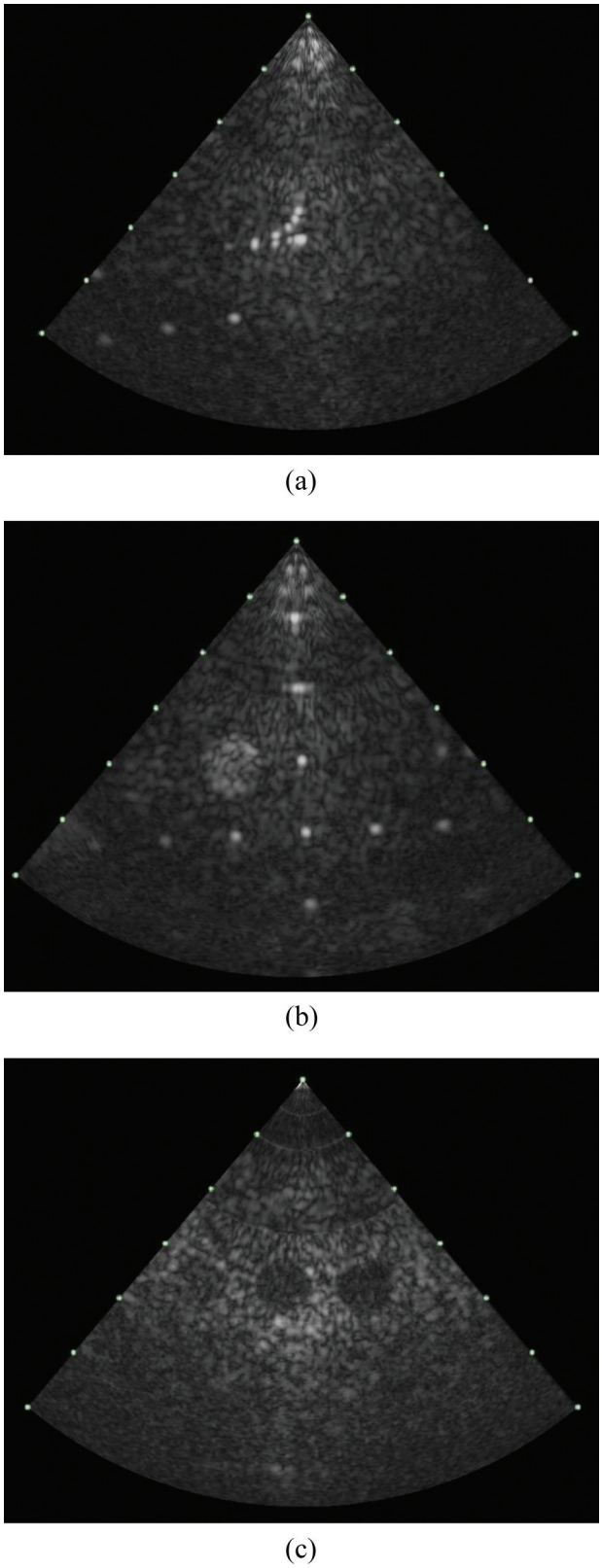

Fig. 9. B-mode images of targets in a tissue phantom obtained using PMUT Array 2 connected to the Duke T5 scanner and operating at 40 Vpp at 4.8 MHz. (a) lateral resolution targets, (b) depth markers and a hyperechoic tumor with +15 dB contrast, and (c) hypoechoic cysts with 8 mm diameter and −3, −6, and −9 dB contrast, respectively.

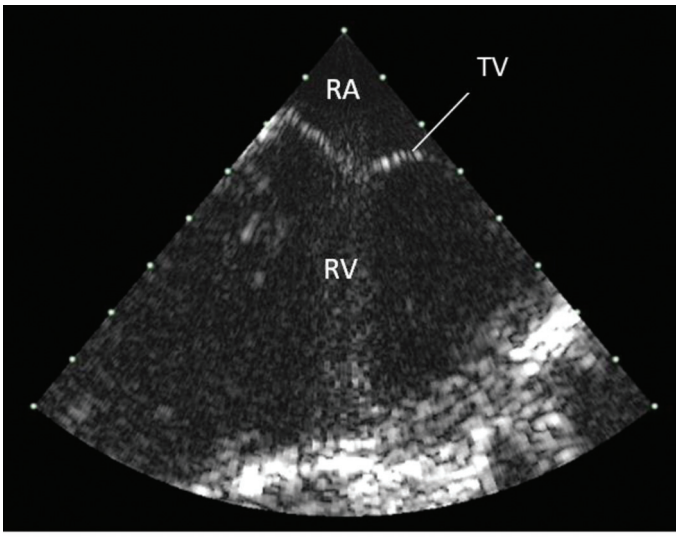

(a)

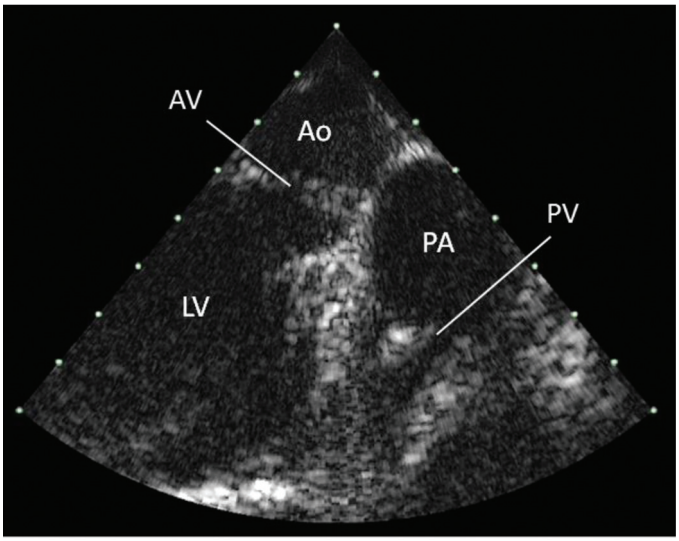

(b)

Fig. 10. *In vivo* B-mode images acquired using PMUT Array 2 operating at 5 MHz with the V360 system and positioned in the right atrium (RA) of a porcine model. (a) Image of tricuspid valve (TV) and right ventricle (RV). (b) Image of the aorta (Ao), aortic valve (AV), pulmonary artery (PA), pulmonary valve (PV), and left ventricle (LV).

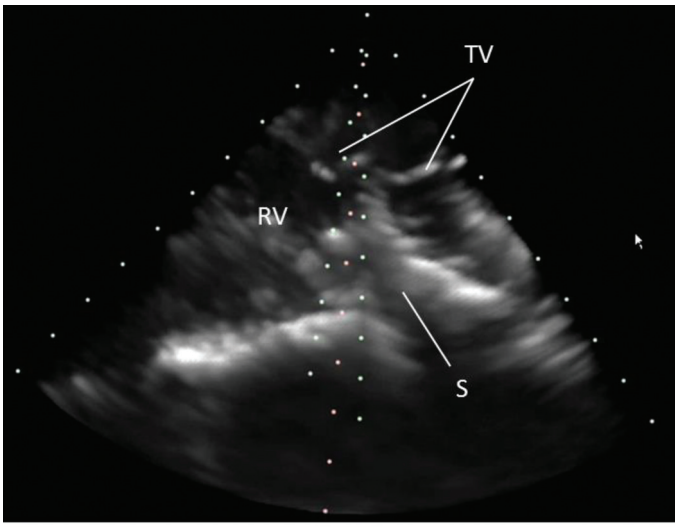

(a)

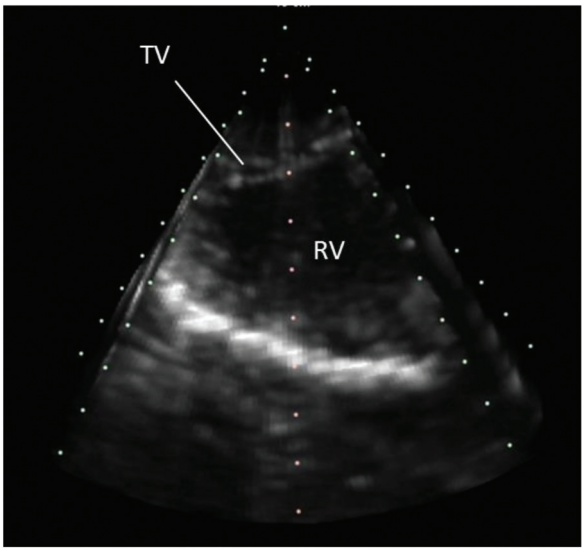

(b)

Fig. 11. *In vivo* real-time volume renderings acquired using PMUT Array 2 operating at 5 MHz with the V360 system and positioned in the right atrium of a porcine model. Views of the right ventricle (RV), tricuspid valve (TV), and interventricular septum (S), including: (a) anterior coronal (left face of pyramid in image) and sagittal (right face of pyramid) views, (b) posterior coronal view. The real-time segment is provided as a multimedia attachment.

PMUT transmit output and receive signal were also increased with more membranes contributing to the performance of each element.

A transmit pulse from one element of Array 2 was measured in a water tank with an Onda GL-0200 hydrophone at 20 mm range. The element was excited with a 3-cycle sine wave pulse at 30 V_{pp}, and the received signal before amplification is shown in Fig. 8(a). The frequency spectrum obtained by fast Fourier transform (FFT) of the transmit pulse is shown in Fig. 8(b) with −6-dB bandwidth of 30%. B-mode images were obtained using the 64 × 4 array connected to the T5 system. Fig. 9 shows images of targets in a tissue phantom (040GSE, Computerized Imaging Reference Systems Inc., Norfolk, VA) with 0.5 dB/cm-MHz attenuation. Array elements were driven at 40 V_{pp} at 4.8 MHz. As shown in Fig. 9(a), lateral resolution targets with spacing down to 1 mm were resolved at approximately 3 cm depth, and axial spacing down to 0.5 mm was resolved. Fig. 9(b) shows depth markers imaged to 6 cm depth as well as a hyperechoic tumor with +15 dB contrast. Fig. 9(c) shows hypoechoic cysts with 8 mm diameter and −3, −6 and −9 dB contrast, respectively.

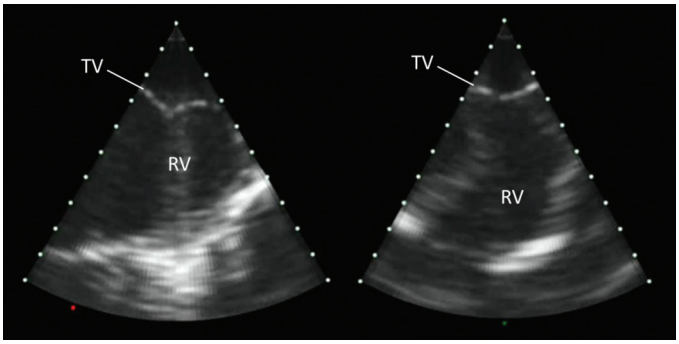

Fig. 12. *In vivo* real-time simultaneous B-mode views acquired using PMUT Array 2 operating at 5 MHz with the V360 system and positioned in the right atrium of a porcine model. Views of the right ventricle (RV) and tricuspid valve (TV), including anterior coronal view (left) and sagittal view (right).

B. In Vivo Imaging Experiments

In vivo images were obtained in an adult swine using PMUT Array 2 connected to the V360 prototype volume ultrasound scanner and associated in-line amplifiers. The PMUT array was driven with 3-cycle sine wave pulses at 45 V_{pp} at 5 MHz. The catheter was inserted through a 14-Fr introducer sheath in the femoral vein and advanced through the inferior vena cava and into the right atrium. The catheter tip was deflected caudally to view regions around the right and left ventricles. Fig. 10 shows B-mode images with views of the tricuspid, aortic, and pulmonary valves. Fig. 11 shows individual still images captured from a real-time volume sequence of the right ventricle and tricuspid valve imaged from the right atrium. Volume sector was 60° × 60° with 10 cm scan depth captured at a frame rate of 26 volumes per second. The frame rate could be increased to 31 volumes per second by reducing scan depth to 8 cm. The V360 performed 16:1 receive parallel processing to achieve high frame rate for the real-time volume rendering. Fig. 12 also shows simultaneous orthogonal B-mode views of the tricuspid valve and right ventricle.

IV. Conclusion

Real-time 3-D intracardiac ultrasound catheters containing PMUT matrix arrays were fabricated with through-silicon interconnects to facilitate electrical connection to both the PMUT elements and ground layer from the back surface of the PMUT substrate. Mating cable assemblies with silicon termination substrates were thermo-compression bonded to the PMUT substrates to enable wire connection to the PMUT substrate contacts without significant increase in array footprint or other additional interconnect means such as wirebonding. The interconnected PMUT arrays were assembled into 14-Fr side-viewing catheters capable of transfemoral insertion into the right atrium for intracardiac imaging.

In vivo real-time 3-D ultrasound imaging in a porcine model was achieved using these novel PMUT arrays. To our knowledge, this the first report of either *in vivo* or real-time 3-D imaging using a PMUT transducer. A PMUT array with rectangular aperture containing 256 active elements was used for intracardiac imaging. Although elevation resolution was limited, the 64 × 4 array operating at 5 MHz was capable of real-time 3-D imaging. The array contained four PMUT membranes per element, which reduced element impedance and increased transmit and receive signals compared with previous designs. Resolution and image quality could be improved by providing 512 (64 × 8) array elements, increasing elevation aperture where possible based on catheter lumen diameter, and increasing array frequency to 8 to 10 MHz. Catheter-compatible cabling with 512 signal wires was demonstrated in this work using a 32 × 16 PMUT array for *in vitro* imaging. Using the V360 ultrasound system, real-time volume rendered images of cardiac anatomy were acquired with 60° × 60° volume sector at 8 to 10 cm scan depth and frame rate of up to 31 volumes per second.

Acknowledgments

The authors thank M. Hunt and A. Stewart from RTI for their cable fabrication work; G. Kirwan and L. Vo of RTI and A. Iranian of Cartika Medical for their work on design of the intracardiac catheters; D. Shah and S. Kumar from Duke University for their assistance with PMUT device testing; and Dr. P. Wolf of Duke University for performing the animal surgery for intracardiac ultrasound imaging.

References

[1] E. Altiok, R. Koos, J. Schröder, K. Brehmer, S. Hamada, M. Becker, A. H. Mahnken, M. Almalla, G. Dohmen, R. Autschbach, N. Marx, and R. Hoffmann, "Comparison of two-dimensional and three-dimensional imaging techniques for measurement of aortic annulus diameters before transcatheter aortic valve implantation," *Heart*, vol. 97, no. 19, pp. 1578–1584, 2011.

[2] N. Bogunovic, L. Faber, W. Scholtz, K. P. Mellwig, D. Horstkotte, and F. van Buuren, "Real-time three-dimensional transoesophageal echocardiography during percutaneous transcatheter occlusion of mitral periprosthetic paravalvular leak," *Eur. J. Echocardiogr.*, vol. 12, no. 3, art. no. E27, 2011.

[3] A. P. Lee, Y. Lam, G. W. Yip, R. M. Lang, Q. Zhang, and C. M. Yu, "Role of real time three-dimensional transesophageal echocardiography in guidance of interventional procedures in cardiology," *Heart*, vol. 96, no. 18, pp. 1485–1493, 2010.

[4] S. Ali, L. K. George, P. Das, and S. K. G. Koshy, "Intracardiac echocardiography: Clinical utility and application," *Echocardiography*, vol. 28, no. 5, pp. 582–590, 2011.

[5] F. F. Faletra, F. Regoli, M. Acena, and A. Auricchio, "Value of real-time transesophageal 3-dimensional echocardiography in guiding ablation of isthmus-dependent atrial flutter and pulmonary vein isolation," *Circ. J.*, vol. 76, no. 1, pp. 5–14, 2012.

[6] T. Moukabary, F. F. Faletra, I. Kronzon, W. Thomas, and V. L. Sorrell, "Three-dimensional echocardiography in the electrophysiology laboratory," *Echocardiography*, vol. 29, no. 1, pp. 117–122, 2012.

[7] D. Garcıa-Fuertes, D. Mesa-Rubio, M. Ruiz-Ortiz, M. Delgado-Ortega, I. Tejero-Mateo, M. Pan-Alvarez-Ossorio, J. Suarez-de-Lezo, and M. Lafuente, "Monitoring complex secundum atrial septal defects percutaneous closure with real time three-dimensional echocardiography," *Echocardiography*, vol. 29, no. 6, pp. 729–734, 2012.

[8] D. P. Perrin, N. V. Vasilyev, G. R. Marx, and P. J. del Nido, "Temporal enhancement of 3-D echocardiography by frame reordering," *JACC Cardiovasc. Imaging*, vol. 5, no. 3, pp. 300–304, 2012.
[9] S. S. Kuppahally, S. E. Litwin, L. S. Green, S. M. Ishihara, R. A. Freedman, and A. D. Michaels, "Utility of intracardiac echocardiography for atrial baffle leak closure in repaired transposition of the great arteries," *Echocardiography*, vol. 27, no. 8, pp. E90–E93, 2010.
[10] J. E. Banchs, P. Patel, G. V. Naccarelli, and M. D. Gonzalez, "Intracardiac echocardiography in complex cardiac catheter ablation procedures," *J. Interv. Card. Electrophysiol.*, vol. 28, no. 3, pp. 167–184, 2010.
[11] R. Fontes-Carvalho, F. Sampaio, J. Ribeiro, and V. G. Ribeiro, "Three-dimensional intracardiac echocardiography: A new promising imaging modality to potentially guide cardiovascular interventions," *Eur. Heart J. Cardiovasc. Imaging*, vol. 14, no. 10, p. 1028, 2013.
[12] A. Al Ahmad, K. Chia, J. Evans, J. Schoenhard, M. Harwood, M. Perez, P. Zei, H. Hsia, and P. Wang, "3-D intracardiac echocardiography in left atrial ablation," *J. Cardiovasc. Electrophysiol.*, vol. 22, p. S43, 2011.
[13] W. Lee, W. Griffin, D. Wildes, D. Buckley, T. Topka, T. Chodakauskas, M. Langer, S. Calisti, S. Bergstoe, J.-P. Malacrida, F. Lanteri, J. Maffre, B. McDaniel, K. Shivkumar, J. Cummings, D. Callans, F. Silvestry, and D. Packer, "A 10-Fr ultrasound catheter with integrated micromotor for 4-D intracardiac echocardiography," *IEEE Trans. Ultrason. Ferroelectr. Freq. Control*, vol. 58, no. 7, pp. 1478–1491, 2011.
[14] S. W. Smith, E. D. Light, S. F. Idriss, and P. D. Wolf, "Feasibility study of real-time three-dimensional intracardiac echocardiography for guidance of interventional electrophysiology," *Pacing Clin. Electrophysiol.*, vol. 25, no. 3, pp. 351–357, 2002.
[15] W. Lee, S. F. Idriss, P. D. Wolf, and S. W. Smith, "A miniaturized catheter 2-D array for real-time, 3-D intracardiac echocardiography," *IEEE Trans. Ultrason. Ferroelectr. Freq. Control*, vol. 51, no. 10, pp. 1334–1346, 2004.
[16] A. Moini, A. Nikoozadeh, O. Oralkan, J. W. Choe, A. F. Sarioglu, D. N. Stephens, A. de la Rama, P. Chen, C. Chalek, A. Dentinger, D. Wildes, L. S. Smith, K. Thomenius, K. Shivkumar, A. Mahajan, M. O'Donnell, D. J. Sahn, and P. T. Khuri-Yakub, "Volumetric intracardiac imaging using a fully integrated cMUT ring array: Recent developments," in *Proc. IEEE Ultrasonics Symp.*, 2011, pp. 692–695.
[17] B. T. Khuri-Yakub and O. Oralkan, "Capacitive micromachined ultrasonic transducers for medical imaging and therapy," *J. Micromech. Microeng.*, vol. 21, no. 5, pp. 54004–54014, 2011.
[18] X. Zhuang, A. S. Ergun, Y. Huang, I. O. Wygant, O. Oralkan, and B. T. Khuri-Yakub, "Integration of trench-isolated through-wafer interconnects with 2-D capacitive micromachined ultrasonic transducer arrays," *Sens. Actuators A*, vol. 138, no. 1, pp. 221–229, 2007.
[19] W. Lee and S. W. Smith, "Intracardiac catheter 2-D arrays on a silicon substrate," *IEEE Trans. Ultrason. Ferroelectr. Freq. Control*, vol. 49, no. 4, pp. 415–425, 2002.
[20] D. Akai, T. Yogi, I. Kamja, Y. Numata, K. Ozaki, K. Sawada, N. Okada, K. Higuchi, and M. Ishida, "Miniature ultrasound acoustic imaging devices using 2-D PMUTS array on epitaxial PZT/Sr-RuO_3/Pt/γ-Al_2O_3/Si Structure," in *Proc. IEEE Transducers*, 2011, pp. 910–913.
[21] F. Griggio, C. E. M. Demore, H. Kim, J. Gigliotti, Y. Qiu, T. N. Jackson, K. Choi, R. L. Tutwiler, S. Cochran, and S. Trolier-McKinstry, "Micromachined diaphragm transducers for miniaturised ultrasound arrays, in *Proc. IEEE Ultrasonics Symp.*, 2012, pp. 1–4.
[22] Y.-F. Wang, T.-L. Ren, Y. Yang, H. Chen, C.-J. Zhou, L.-G. Wang, and L.-T. Liu, "High-density PMUT array for 3-D ultrasonic imaging based on reverse-bonding structure," in *Proc. IEEE MEMS*, 2011, pp. 1035–1038.
[23] D. E. Dausch, J. B. Castellucci, K. H. Gilchrist, J. R. Carlson, D. R. Chou, and O. T. von Ramm, "Improved pulse-echo imaging performance for flexure-mode PMUT arrays," in *Proc. IEEE Ultrasonics Symp*, 2010, pp. 451–454.
[24] D. E. Dausch, C. Gregory, and R. L. Rhoades, "Pt vias for high temperature MEMS interconnects," in *Proc. Int. Interconnect Technology Conf.*, 2010, pp. 1–3.
[25] G. H. Haertling, "An acetate precursor process for bulk and thin film PLZT," in *Proc. IEEE 7th Int. Symp. Applications of Ferroelectrics*, 1990, pp. 292–295.
[26] R. A. Miller and J. J. Bernstein, "A novel wet etch for patterning lead zirconate-titanate (PZT) thin films," *Integr. Ferroelectr.*, vol. 29, no. 3–4, pp. 225–231, 2000.
[27] G. Gurun, P. Hasler, and F. L. Degertekin, "Front-end receiver electronics for high-frequency monolithic CMUT-on-CMOS imaging arrays," *IEEE Trans. Ultrason. Ferroelectr. Freq. Control*, vol. 58, no. 8, pp. 1658–1668, 2011.
[28] D. E. Dausch, J. B. Castellucci, D. R. Chou, and O. T. von Ramm, "Theory and operation of 2-D array piezoelectric micromachined ultrasound transducers," *IEEE Trans. Ultrason. Ferroelectr. Freq. Control*, vol. 55, no. 11, pp. 2484–2492, 2008.

David E. Dausch (M'05–SM'07) received B.S. (magna cum laude) and Ph.D. degrees in ceramic engineering from Clemson University, Clemson, SC, in 1991 and 1995, respectively. From 1995 to 1997, he served as a postdoctoral research associate for the National Research Council at NASA Langley Research Center in Hampton, VA, where he studied mechanical stress effects on piezoelectric materials, electro-mechanical fatigue properties of piezoelectric actuators, and their application in aeronautic systems. He joined the Microelectronics Center of North Carolina (MCNC), Research Triangle Park, NC, as an Electronic Materials Engineer in 1998, and then Principal Research Engineer and Team Leader of the Sensors & Actuators Group in 2001. He joined RTI International, Research Triangle Park, NC, in 2005, and currently serves as Technical Director in the Electronics and Applied Physics Division. Dr. Dausch has managed numerous R&D programs related to microelectromechanical systems (MEMS) technologies and applications. He was awarded a Best Cardiovascular Innovation Award at Cardiovascular Research Technologies (CRT) 2013 for the development of real-time 3-D intracardiac echo catheters based on PMUT matrix arrays. Dr. Dausch has authored 35 research publications and holds 15 U.S. patents.

Kristin H. Gilchrist received a B.E. degree (summa cum laude) in biomedical engineering and electrical engineering from Vanderbilt University, Nashville, TN, in 1997; an M.S. degree in electrical engineering from Stanford University, Stanford, CA, in 1999; and a Ph.D. degree in electrical engineering from Stanford University in 2003. Dr. Gilchrist is currently a Research Scientist in the Electronics and Applied Physics Division at RTI International. Her technical expertise includes the development of novel microfabricated devices and the analysis of biological signals. She currently manages a program to develop a seizure monitor for children with epilepsy, and is developing an *in vitro* cardiotoxicity screening platform using microelectrode array recording of cardiomyocytes. She served as the lead fabrication engineer for development of PMUT arrays for a real-time, 3-D intracardiac imaging catheter. Other projects that she has supported include the development of MEMS vacuum electronic devices, optical scanning mirrors for endoscopic imaging applications, and microfluidic devices. Her work has appeared in many peer-reviewed journals, including *Applied Physics Letters*, *Biomicrofluidics*, the *Journal of Micromechanics and Microengineering*, and *Sensors and Actuators*. She has several U.S. patents and patent applications.

James B. Carlson received B.S. degrees in mechanical and electrical engineering from North Carolina State University, Raleigh, NC, in 1983. Mr. Carlson is a Senior Research Scientist in RTI International's Electronics & Applied Physics Division, where he has focused on developing low-power handheld embedded system designs, mixed-mode MEMS control ASICs, and the development and transitioning of developed devices and systems into products. His career spans more than 25

years in research and development with involvement in both mechanical and electrical designs. He has worked in the telephony and datacom industries, performing designs that encompassed tamper-evident FIPS-140 system designs, redundant systems, microprocessors, microcontrollers, data encryption ASICs, as well as outsource production process development. His specialties include system architecture; chip-, board-, and system-level hardware design; production; and regression test system development. He has extensive experience with high-voltage mixed-signal ASIC design/layout, Verilog coding, electronic packaging, machine design, embedded firmware development, microprocessor/microcontroller designs, and safety/security-compliant standards. He was recently awarded an R&D 100 award for the development of the Micro Personal Exposure Monitor. He is also an Adjunct Lecturer teaching Introduction to Embedded Systems at North Carolina State University.

Stephen D. Hall received a B.A. degree in humanities from North Carolina State University in Raleigh, NC, in 1985. He has completed multiple US Naval service schools with concentrations in electronic, electromechanical, and microwave generation systems. His career includes more than 15 years of experience in wafer-level semiconductor manufacturing, die-level packaging, and device testing operations. Past employers include Motorola, JDS Uniphase, MEMSCAP, Unitive, and Amkor Technology. He also has a variety of experience in manufacturing equipment engineering, maintenance and repair. He joined RTI International in 2009, and his current position as an Engineer in the Electronics and Applied Physics Division has led to assignments including the assembly and testing of real-time 3-D intracardiac echo catheters, microfluidic devices, personal exposure monitors, and a variety of other surface-mount PC-board assemblies.

John B. Castellucci was born in Englewood, NJ, on July 18, 1959. He received his B.S.E. and M.S. degrees in biomedical engineering from Duke University in Durham, NC, in 1981 and 1986, respectively.

From 1985 through 1986, he worked as a Senior Antenna Engineer for Channel Master Satellite Systems in Smithfield, NC, designing C- and Ku-band satellite dishes. From 1986 through 1988, he worked as a Senior Design Engineer for Corazonix Corporation in Oklahoma City, OK, developing signal-averaging electrocardiograph and cardiac output monitoring instrumentation. Since then, he has worked as a Research Associate in the Diagnostic Ultrasound Laboratory at Duke University, developing advanced ultrasonic imaging scanners and transducers. He also serves as a consultant for industry. His research interests include diagnostic imaging systems, 3-D flow measurement and visualization, micro-machined transducers, and 2-D and high-frequency arrays.

Olaf T. von Ramm was born in Posen, Poland, on August 16, 1943. He received B.A.Sc. and M.A.Sc. degrees in electrical engineering from the University of Toronto, Toronto, ON, Canada, in 1968 and 1970, respectively, and a Ph.D. degree in biomedical engineering from Duke University in Durham, NC, in 1973.

Dr. von Ramm joined the faculty of Duke University in 1974 and currently is the Thomas Lord Professor of Engineering, Professor of Biomedical Engineering, and Professor of Medicine. He has served a variety of administrative roles at Duke University, including Director of Undergraduate Studies, Director of Graduate Studies, Chair of the Engineering Faculty Council, and Department Representative to the University's Academic Council. He is the Director of the National Science Foundation sponsored Center for Emerging Cardiovascular Technologies. His research interests include diagnostic ultrasound imaging systems, IR imaging, medical instrumentation, and their new applications. Dr. von Ramm has served in consulting roles for government agencies, industry, and academia.

He is a fellow of the American Institute of Ultrasound in Medicine, the American Society of Echocardiography, and the American Institute for Medical and Biomedical Engineering. He is a 1998 Computerworld Smithsonian Research Collection Awardee.